ChemPubSoc Europe

DOI: 10.1002/chem.201403909

CHEMISTRY
A European Journal
Full Paper

Metal–Organic Frameworks

The First One-Pot Synthesis of Metal–Organic Frameworks Functionalised with Two Transition-Metal Complexes

Ana E. Platero-Prats,[a, b, c] Antonio Bermejo Gómez,[a, b] Louise Samain,[c] Xiaodong Zou,*[a, c] and Belén Martín-Matute*[a, b]

Abstract: The synthesis of a metal–organic framework (UiO-67) functionalised simultaneously with two different transition metal complexes (Ir and Pd or Rh) through a one-pot procedure is reported for the first time. This has been achieved by an iterative modification of the synthesis parameters combined with characterisation of the resulting materials using different techniques, including X-ray absorption spectroscopy (XAS). The method also allows the first synthesis of UiO-67 with a very wide range of loadings (from 4 to 43 mol%) of an iridium complex ($[IrCp^*(bpydc)(Cl)Cl]^{2-}$; bpydc = 2,2′-bipyridine-5,5′-dicarboxylate, Cp* = pentamethylcyclopentadienyl) through a pre-functionalisation methodology.

Introduction

Metal–organic frameworks (MOFs) are modular and crystalline materials[1] amenable to chemical modification[2] that can be used in a wide range of applications.[3] When the intrinsic properties of MOFs are combined with those of transition metal complexes,[4] crystalline materials with multiple potential uses, including catalysis, are created. MOFs were originally functionalised by introducing organic fragments into their linkers.[5] Recently, a multivariate (MTV) functionalisation was reported, through which a large number of diverse linkers bearing different organic functional groups were incorporated into MOF-5.[6] Another versatile approach is the linker-exchange method, for example, post-synthetic exchange (PSE) and solvent-assisted linker exchange (SALE).[7]

MOFs can be functionalised with transition metal complexes through post- or pre-functionalisation strategies. Examples of post-functionalisation include metal impregnations and metallations.[8] In the past few years, pre-functionalisation strategies have emerged as a versatile methodology, whereby modified transition metal complexes (metallo-linkers) serve as building blocks for MOF synthesis.[9] In this context, Lin and co-workers reported a "mix-and-match" strategy, in which a mixture of unfunctionalised linkers and metallo-linkers with matching length and connectivity was incorporated into the same MOF.[10] Cohen, Ott, and co-workers have recently reported similar results using the PSE protocol.[11]

Despite great efforts, the synthesis of transition-metal-functionalised MOFs still presents a challenge. This is partly due to decomposition of transition metal complexes under the reaction conditions needed for MOF synthesis. The controlled synthesis of these materials functionalised with a wide range of loadings of a transition metal or with more than one transition metal complex is difficult but desirable. Furthermore, little is known about how functionalisation may change the structure of MOFs. Herein, we report the first one-pot synthesis of MOFs functionalised with one or simultaneously two transition metal complexes from their basic components (i.e., transition metal precursors, linkers, and structural metal salts) (Figure 1). The method is exemplified with the Zr^{IV} MOF UiO-67[12] and transition metal complexes **LM1** = $[IrCp^*(bpydc)(Cl)Cl]^{2-}$, **LM2** = $[Pd(bpydc)Cl_2]^{2-}$, and **LM3** = $[RhCp^*(bpydc)(Cl)Cl]^{2-}$ (**L** = bpydc = 2,2′-bipyridine-5,5′-dicarboxylate).[13]

Results and Discussion

The molecular formula of UiO-67 is $[Zr_6O_4(OH)_4(bpdc)_6]$, with six unique linkers (bpdc = 4,4′-biphenyldicarboxylate) per octahedral (O_h) cavity. Functionalised analogues can then be defined as $[Zr_6O_4(OH)_4(bpdc)_{6-y}(\mathbf{LM1})_y]$, in which y is the number of metallo-linkers (**LM1**) per O_h cavity (Figure 2). As an example, 33 mol% functionalisation would be represented by $y = 2$ (Figure 2). The parameter y' is then defined as the intended number of metallo-linkers per O_h cavity (see the Experimental

[a] Dr. A. E. Platero-Prats,[+] Dr. A. Bermejo Gómez,[+] Prof. X. Zou, Prof. B. Martín-Matute
Berzelii Center EXSELENT on Porous Materials
Stockholm University
10691 Stockholm (Sweden)
E-mail: belen@organ.su.se

[b] Dr. A. E. Platero-Prats,[+] Dr. A. Bermejo Gómez,[+] Prof. B. Martín-Matute
Department of Organic Chemistry
Stockholm University
10691 Stockholm (Sweden)

[c] Dr. A. E. Platero-Prats,[+] Dr. L. Samain, Prof. X. Zou
Department of Materials and Environmental Chemistry
Stockholm University
10691 Stockholm (Sweden)

[+] These authors contributed equally to this work.

Supporting information for this article is available on the WWW under http://dx.doi.org/10.1002/chem.201403909.

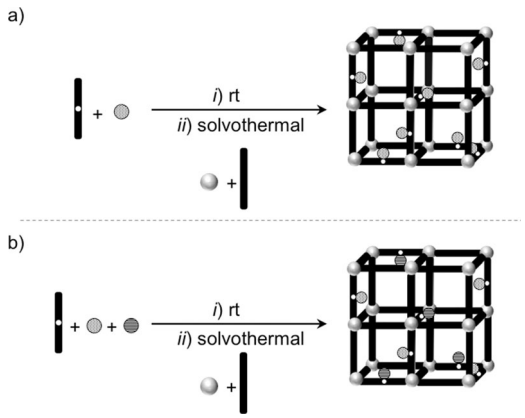

Figure 1. One-pot synthesis of UiO-67 functionalised with a) one metal complex or b) simultaneously multifunctionalised with two. The grey spheres correspond to the zirconium clusters. The dotted and striped spheres correspond to different metal complexes. The bpdc = 4,4′-biphenyl dicarboxylate linkers are represented as black rods and the bpydc = 2,2′-bipyridine-5,5′-dicarboxylate linkers as black rods with white dots.

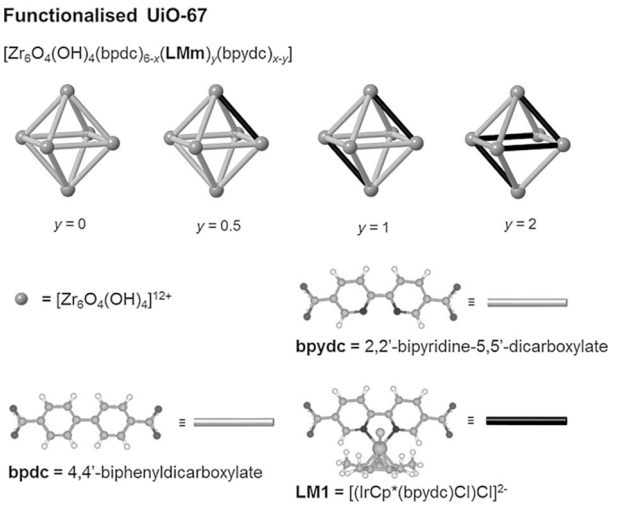

Figure 2. The UiO-67 composition is described as $[Zr_6O_4(OH)_4L_6]$, with six linkers per $[Zr_6O_4(OH)_4]^{12+}$ cluster. Among the six linkers (L) are $(6-x)$ bpdc linkers, $(x-y)$ demetallated **LM1** linkers (i.e., bpydc), and y functionalised metallo-linkers **LMm** (m = 1–3, 1 = Ir, 2 = Pd, 3 = Rh). The composition of the O_h cavity in UiO-67 is $[Zr_{36}O_{24}(OH)_{24}L_{12}]$. Each linker is shared by two O_h cavities and the number of metallo-linkers per O_h cavity is represented by y.

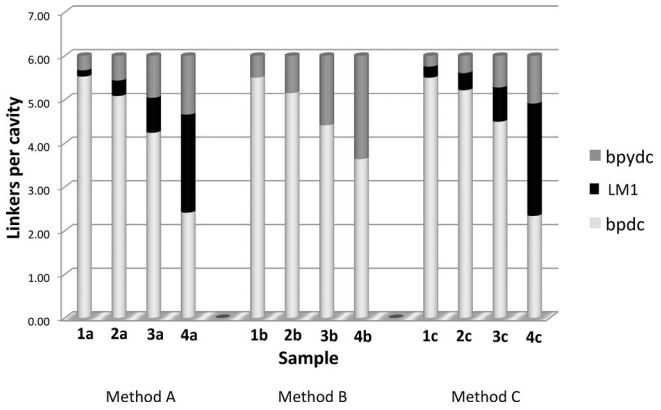

Figure 3. Linker composition per O_h cavity.

Table 1. LM1 and bpydc contents determined by ^{1}H NMR spectroscopy for MOFs synthesised using Methods A, B, and C, in terms of degree of functionalisation per O_h cavity (y).

	Sample (Method)[a,b]	bpdc[c]	bpydc[c]	**LM1**[c,d]	**LM1**/ bpydc[e]	Ir [wt%][f]	Isolated yield [%]
1	**1a** (A)	5.53	0.33	0.14	0.42	1.22	58
2	**2a** (A)	5.08	0.56	0.36	0.64	2.79	62
3	**3a** (A)	4.24	0.95	0.81	0.85	5.53	65
4	**4a** (A)	2.41	1.34	2.25	1.68	12.35	87
5	**1b** (B)	5.50	0.50	0	0	0.22	n.d.
6	**2b** (B)	5.51	0.85	0	0	0.51	n.d.
7	**3b** (B)	4.41	1.59	0	0	1.74	n.d.
8	**4b** (B)	3.64	2.36	0	0	5.81	n.d.
9	**1c** (C)	5.50	0.25	0.25	1.00	1.81	77
10	**2c** (C)	5.22	0.39	0.39	1.00	4.51	83
11	**3c** (C)	4.49	0.72	0.79	1.10	7.87	95
12	**4c** (C)	2.34	1.09	2.57	2.36	14.80	97

[a] Method A: 100 °C, Teflon autoclave reactors using dry DMF as the solvent and 5 equiv of H_2O. Method B: 140 °C, Teflon autoclave reactors using dry DMF as the solvent and 5 equiv of H_2O. Method C: 100 °C, sealed microwave tube in an oil bath with stirring using dry DMF as the solvent and 5 equiv of H_2O. [b] Intended **LM1** amounts (y') for samples **1a**–**1c**, **2a**–**2c**, **3a**–**3c**, and **4a**–**4c** were 0.5, 1, 2, and 4, respectively. [c] Determined by ^{1}H NMR spectroscopic analysis of the digested samples. [d] Number of metallo-linkers (**LM1**) per O_h cavity (y). [e] The value **LM1**/bpydc was consistent for different batches. [f] Determined by ICP-AES analysis.

Section). First, we evaluated the effect of several synthetic parameters in the preparation of UiO-67 functionalised with **LM1** (from Zr^{IV} salts, H_2bpdc, and H_2**LM1**),[10] with the aim of obtaining materials with a wide range of iridium loadings. We found that the crystallinity of UiO-67 functionalised with **LM1** ($y' = 1$) is highly dependent on the amount of water used in the synthesis. By varying the number of equivalents of water (from 3 to 150 equiv per $ZrCl_4$), we found that 5 equiv gave crystalline samples (Figure 3 and Table 1, entry 2, $y = 0.36$; Supporting Information). Water was needed to form the Zr cluster. Although 1.3 equiv per Zr would be theoretically sufficient (in agreement with the molecular formula $[Zr_6O_4(OH)_4(bpdc)_{6-y}(\mathbf{LM1})_y]$, a slight excess of H_2O was needed to obtain good reproducibility. The use of $ZrOCl_2$ instead of $ZrCl_4$ resulted in poorer crystallinity (see the Supporting Information). In addition, decomposition of the iridium complex was observed when different additives (e.g., formic acid or potassium carbonate) were used. To obtain a methodology that would allow higher iridium loadings, different **LM1** concentrations and synthesis temperatures (100 °C, Method A; 140 °C, Method B) were then tested. In all cases (Table 1, entries 1–8), crystalline materials were obtained (Figure 4). ICP-AES showed that the iridium contents were systematically lower at higher temperatures (Table 1, entries 1–4 vs. 5–8). The amount of **LM1** was determined by analysing the samples by ^{1}H NMR spectroscopy after digestion under optimized conditions (i.e., $[D_6]DMSO/D_3PO_4$; see the Supporting In-

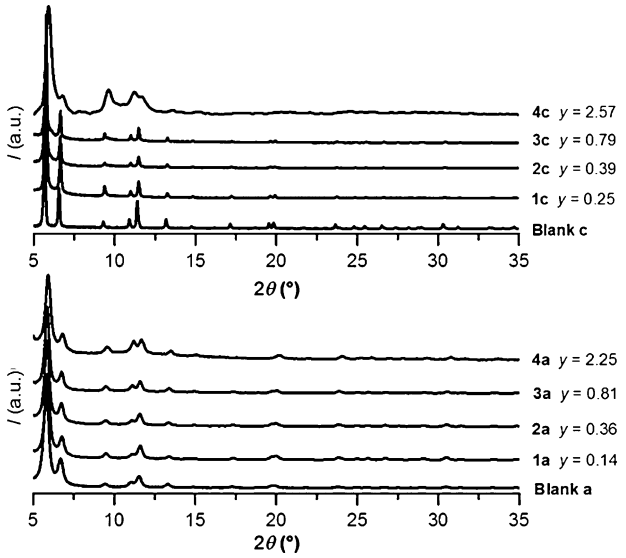

Figure 4. Powder X-ray diffraction patterns collected from samples **Blank a**, **1a**–**4a**, **Blank c**, and **1c**–**4c**.

formation). Surprisingly, H_2bpydc was found in all digested samples. Free bpydc was formed by demetallation of **LM1** during the synthesis of the MOFs, lowering the iridium metallo-linker content in the products (Table 1).[14] Furthermore, although samples **1b**–**4b** contained iridium (as confirmed by ICP-AES), no **LM1** was found in the digested samples by ^{1}H NMR spectroscopy (Table 1, entries 5–8). Iridium is thus not present as Ir^{III} coordinated to bpydc but as other species, which was further confirmed by XAS (see below).

Next, we explored the effect of stirring during the synthesis of the MOF, with the aim of decreasing demetallation of **LM1** and increasing the yield. The reaction mixtures were stirred in sealed vials and heated in an oil bath at 100 °C (Method C).

Stirring resulted in a more homogeneous reaction mixture, preventing both high local concentrations of acidic species (e.g., HCl) and local overheating,[20] which may have resulted in reduced demetallation. Indeed, ^{1}H NMR spectroscopic analysis after digestion of the samples showed that **1c**–**4c** had undergone significantly lower demetallation compared to the products obtained without stirring at the same temperature (**1a**–**4a**) and, importantly, their crystallinity was not affected. The **LM1**/bpydc ratios were 1.00, 1.00, 1.10, and 2.36 for **1c**–**4c** (Table 1, entries 9–12; Supporting Information), compared to 0.42, 0.64, 0.85, and 1.68 for **1a**–**4a** (Table 1, entries 1–4). This represents increases in the **LM1**/bpydc ratio by 138, 56, 29, and 40%, respectively. Furthermore, not only was the degree of functionalisation better controlled, but the yields were considerably higher (by 10–30%). PXRD showed that Methods A and C gave UiO-67 materials with good crystallinity and a wide degree of functionalisation (y = 0–2.25) (Figure 4; Supporting Information). Interestingly, synthesis with stirring (**1c**–**3c**) led to sharper PXRD peaks than without stirring, although significant peak broadening was observed for the highest functionalisation (**4c**, y = 2.57). This could be explained by the formation of defects in the crystal structure of the MOF (e.g., domains).

The local environment and oxidation state of iridium was investigated by XAS. Figure 5a shows the iridium L_{III}-edge X-ray absorption near-edge structure (XANES), which confirms incorporation of **LM1** in MOFs **3a** and **4a** (**3a**, y = 0.81; **4a**, y = 2.25) and MOFs **3c** and **4c** (**3c**, y = 0.79; **4c**, y = 2.57). The extended

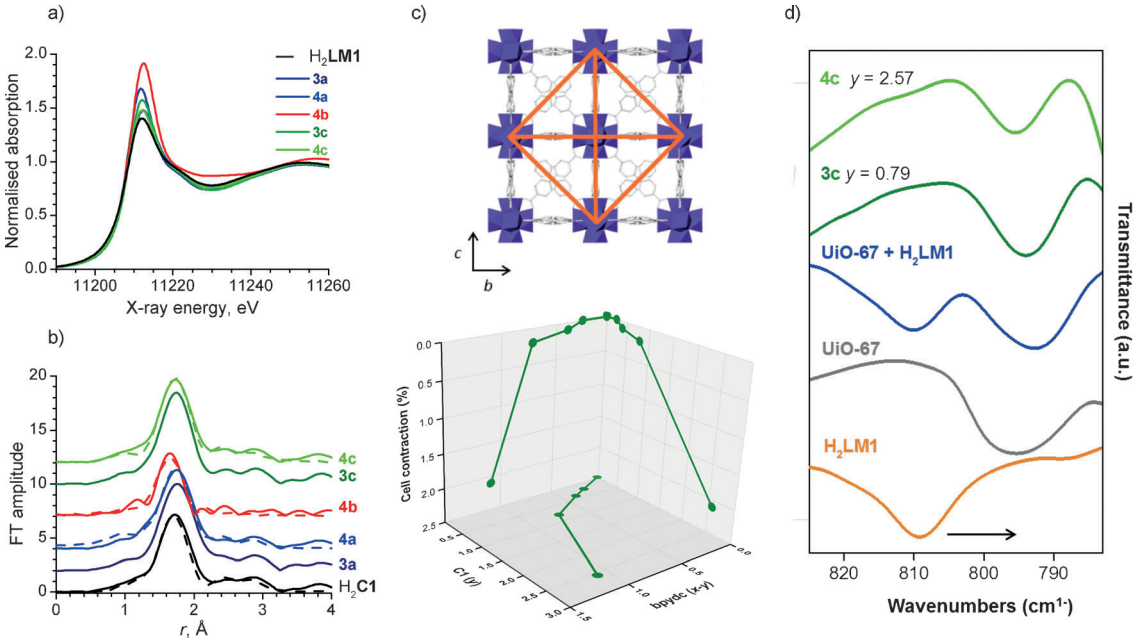

Figure 5. a) Ir L_{III}-edge XANES spectra of H_2**LM1**, **3a**, **4a**, **4b**, **3c**, and **4c**. b) Experimental (solid line) and fitted (dashed line) FT[$\chi(k)\cdot k^3$] functions (bottom) with $\Delta k \approx 2$–12 Å^{-1}. c) UiO-67 crystal structure and 3D plot showing the contraction of the unit cell as a function of **LM1** and bpydc content for MOFs **1c**, **2c**, **3c**, and **4c**, determined from the PXRD data using the Pawley method. d) The ATR/FTIR spectra of H_2**LM1**, UiO-67, a physical mixture of UiO-67 and H_2**LM1**, and functionalised MOFs **3c** and **4c**.

X-ray absorption fine structure (EXAFS) data for H_2**LM1** were fitted using the structure model determined by single-crystal X-ray diffraction (see the Supporting Information). EXAFS analyses on **3a**, **4a**, **3c**, and **4c** confirmed incorporation of iridium exclusively in the form of **LM1** (Figure 5b). In contrast, XANES and EXAFS spectra of **4b** showed the presence of IrO_2 as the major phase, as well as other iridium species such as $IrCl_3$ (see the Supporting Information).

PXRD data of the samples prepared by Method C (**1c**–**4c**) revealed a framework contraction upon functionalisation, which correlated well with the degree of functionalisation *y* (Figure 5c and Table S6.3.1). A minor cell contraction ($\leq$0.2%) occurred in samples with low **LM1** contents (low *y* values) (**1c**–**3c**, $y<0.8$), whereas a significant cell contraction (2.1%) was observed for the highest degree of functionalisation with the iridium metallo-linker (**4c**, $y=2.57$), as given in Table S6.3.1. This framework contraction can be explained by: (i) the different lengths of the bpdc, bpydc, and **LM1** linkers, and (ii) the presence of intermolecular interactions among the **LM1** subunits within the MOF (C–H···π and C–H···O, see the Supporting Information).

Attenuated total reflection Fourier-transform infrared (ATR/FTIR) spectra of solid samples were collected for UiO-67, H_2**LM1**, and MOFs **1c**–**4c**, as well as for a physical mixture of UiO-67 and H_2**LM1**. The aromatic C–H stretching band of the iridium metallo-linker shifted from 810 (H_2**LM1**) to 795 cm^{-1} in the functionalised MOFs. This can be attributed to the different electronic environment of **LM1** when coordinated to the zirconium clusters in the MOF (Figure 5d). Additionally, thermal gravimetric analysis (TGA) confirmed that **LM1** has a different thermal decomposition profile when incorporated into MOFs **1c**–**4c** (see the Supporting Information). N_2 adsorption measurements confirmed that MOFs **1c**–**4c** remained porous despite functionalisation with **LM1**.

Having demonstrated the beneficial effect of adding 5 equiv of water and synthesising the iridium-functionalised MOFs under stirring at 100 °C, we then attempted their synthesis by a one-pot procedure starting from the basic components (Method D, Figure 6, Table 2). The synthesis starting from commercially available [{IrCp*Cl_2}$_2$] and H_2bpydc was successfully accomplished (see the Experimental Section) and afforded MOF **1d** (Table 2, entry 1, $y=0.36$) with higher crystallinity than when Method C was used, and in excellent isolated yield (74%). This procedure is much simpler and more cost-effective, since isolation of the metallo-linker is no longer needed. The framework composition was determined as $[Zr_6O_4(OH)_4(bpdc)_{5.28}(\mathbf{LM1})_{0.36}(bpydc)_{0.36}]$ (Table 2, entry 1), similar to that of the MOF synthesised by Method C $[Zr_6O_4(OH)_4(bpdc)_{5.22}(\mathbf{LM1})_{0.39}(bpydc)_{0.39}]$ (Table 1, entry 10).

Table 2. Sequential one-pot synthesis and characterisation of MOFs functionalised simultaneously with one or two transition metal complexes.

	Sample (Method D)[a]	bpdc	bpydc	**LMm**[b,c]	Isolated yield [%]
1	**1d**	5.28	0.36	0.36 **LM1**	74
2	**2d**	5.29	0.12	0.19 **LM1** + 0.40 **LM2**	84
3	**3d**	4.86	0.34	0.44 **LM1** + 0.36 **LM3**	71

[a] Method D, sequential one-pot synthesis: 1) dry DMF, rt, 24 h; 2) 5 equiv of H_2O, 100 °C, 40 h. [b] Determined by ^{1}H NMR spectroscopic analysis of the digested samples. [c] Number of metallo-linkers (**LMm**) per O_h cavity (*y*).

Taking advantage of this successful methodology, we applied the sequential one-pot route to synthesise for the first time MOFs functionalised simultaneously with two transition metal complexes, **LM1** + **LM2** (**2d**, Ir + Pd) (Table 2, entry 2), and **LM1** + **LM3** (**3d**, Ir + Rh) (Table 2, entry 3). Using the commercially available metal precursors [{IrCp*Cl_2}$_2$], $PdCl_2$, and [{RhCp*Cl_2}$_2$] (Table 2), crystalline dual-functionalised materials were obtained in excellent yields (**2d**, 84%; **3d**, 71%). The compositions were determined after digestion as $[Zr_6O_4(OH)_4(bpdc)_{5.29}(\mathbf{LM1})_{0.19}(\mathbf{LM2})_{0.40}(bpydc)_{0.13}]$ for **2d** and $[Zr_6O_4(OH)_4(bpdc)_{4.86}(\mathbf{LM1})_{0.44}(\mathbf{LM3})_{0.36}(bpydc)_{0.34}]$ for **3d** (Table 2). ATR/FTIR and TGA data confirmed coordination of the metallo-linkers to the zirconium clusters in MOFs **1d**–**3d**, and the BET surface areas of these materials indicated good porosity (see the Supporting Information).

Conclusion

In conclusion, we have presented here the first one-pot synthesis of a metal–organic framework (UiO-67) pre-functionalised with one or simultaneously two transition metal complexes. This efficient methodology uses commercially available metal precursors ([{IrCp*Cl_2}$_2$], $PdCl_2$, and [{RhCp*Cl_2}$_2$]), and requires neither isolation nor purification of the metallo-linkers, resulting in shorter synthesis times and lower costs. This has been achieved by evaluating how the experimental parameters

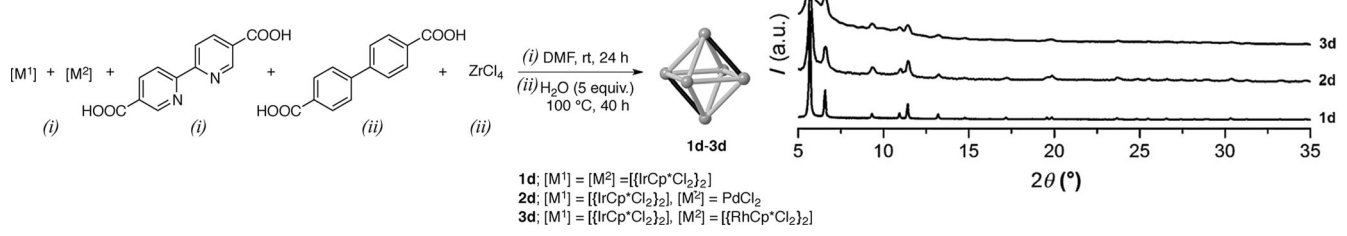

Figure 6. Sequential one-pot synthesis (Method D) of MOFs and PXRD patterns of **1d**, **2d** and **3d**.

(water content, temperature, and stirring) influence the MOF synthesis by means of complementary characterisation techniques (PXRD, ^{1}H NMR, ICP-AES, XAS, TGA, and ATR/FTIR). Additionally, the optimised procedure allows the synthesis of UiO-67 containing an unprecedentedly wide range of iridium loadings (4–43 mol%). This study has also shown that demetallated linkers are part of the MOF structure, and that a framework contraction occurs upon functionalisation.

On the basis of the presented advantages, this sequential one-pot methodology is expected to be broadly applicable for the synthesis of new MOFs functionalised with different transition metal complexes.

Experimental Section

Synthesis of (multi)functionalised UiO-67 MOFs

Synthesis of UiO-67 functionalised with LM1 (Method C): $ZrCl_4$ (46.6 mg, 0.2 mmol, 1 equiv), H_2**LM1** (*z* mmol), and H_2bpdc ([0.2−*z*] mmol) were placed in a vial, dry DMF (9 mL) and water (18 μL, 1 mmol, 5 equiv) were added, and the vial was sealed. The mixture was stirred at room temperature for 10 min, and then it was heated with stirring at 100 °C in an oil bath for 72 h. The reaction mixture was then allowed to cool down to room temperature. The solid was separated by centrifugation, activated by washing sequentially with DMF (15 mL), MeOH (15 mL), water (15 mL), and acetone (15 mL), and dried at 80 °C in vacuum (0.1 mmHg) for 10 h. Note: the value *z* is *y*′ expressed in mmol for a reaction carried out on a 0.2 mmol scale.

One-pot synthesis (Method D): The transition metal complex precursor(s) (0.033 mmol) and H_2bpydc (0.033 mmol) were placed in a microwave tube, dry DMF (9 mL) was added, and the tube was sealed. The mixture was stirred at rt for 24 h. $ZrCl_4$ (0.2 mmol, 1 equiv), H_2bpdc (0.167 mmol), and water (1 mmol, 5 equiv) were then added. The mixture was first stirred at room temperature for 10 min, and then heated under stirring at 100 °C in an oil bath for 72 h. After cooling, the solid was separated by centrifugation, washed sequentially with DMF (15 mL), MeOH (15 mL), water (15 mL), and acetone (15 mL), and dried at 80 °C in vacuum (0.1 mmHg) for 10 h.

Digestion and subsequent molecular analysis of the functionalised MOFs by ^{1}H NMR spectroscopy: Samples were suspended in a 0.1 M solution of D_3PO_4 in D_2O/[D_6]DMSO and stirred at room temperature for 5 h to allow digestion of the MOFs. The solution was then transferred to an NMR tube. ^{1}H NMR spectra were recorded at 500 MHz on a Bruker Advance spectrometer using a BBO S2 probe, 5 mm; with a z-gradient (BBO = broadband observe). In order to minimise the error, the parameters of the acquisition were as follows: number of scans (NS): 200, relaxation delay (D1): 5 s.

X-ray absorption spectroscopy: Ir L_{III}-edge XAS experiments were carried out at the I811 beamline, MAX IV Laboratory, Lund. The spectra were recorded in fluorescence mode because of the relatively low concentrations of Ir in the samples. Data processing and analysis were performed with the Athena and Artemis software package using IFEFFIT.[15,16] The background was removed using the AUTOBK and flattening algorithm implemented in Athena. The pre-edge background was linearly subtracted from 150 to 30 eV below the edge and a three-term polynomial function was used for the post-edge background subtraction over the range 150 to 900 eV above the edge. The frequency cut-off between the background and the data was set at 1.2 Å. The pre-edge background-subtracted spectra were normalised to the edge jump, E0, which was taken as the energy of the first inflection point on the edge, that is, the first maximum in the derivative of the absorption. The EXAFS reduced data $\chi(k)$ were Fourier-transformed into R-space over the range 2–12 Å^{-1} with a k^3 weighting factor and a Hanning window, where the window sill was set at 3 Å^{-1}. The EXAFS function ($\chi(k)$) was then fitted to the ab initio multiple scattering XAS code FEFF in R-space.[17,18] The phase shifts and back-scattering amplitudes were obtained from FEFF6.0 calculations on the structure of metallo-linker H_2**LM1** determined by single-crystal X-ray diffraction analysis. Detailed descriptions of the XAS analyses are given in the Supporting Information.

Powder X-ray diffraction: Powder X-ray diffraction (PXRD) was performed on a Panalytical X'Pert PRO diffractometer in Bragg–Brentano reflection geometry using $Cu_{K\alpha}$ radiation ($\lambda = 1.5418$ Å) at a power of 1800 W (45 kV, 40 mA). The PXRD data were collected using a silicon-based position-sensitive X'Celerator detector and programmed divergence and anti-scattering slits. Samples were suspended in 2-propanol and placed in zero-background sample holders. Optimised counting statistics were obtained by collecting data from the samples using a 0.017° 2θ step scan from 5–35° with an exposure time of 100 s per step. All measurements were performed at room temperature and ambient pressure.

Full-pattern profile-matching using the Pawley method[19] was conducted with Materials Studio using data in the range 2θ = 5–35°. The background was first refined by applying a second-order polynomial function. The profile was calculated starting from the unit cell parameters of CCDC-889530 ($a = 27.0942$ Å, *F*23 space group). Unit cells and the zero-shift were first refined. The background was first refined by applying a tenth-order polynomial function. The patterns were then refined using a pseudo-Voigt profile, followed by refinement of peak asymmetry using the Finger–Cox–Jephcoat asymmetry function. Refinements of unit cell parameters, zero shift, peak asymmetry, and background were used to obtain the final profiles.

Acknowledgements

This project was supported by the Knut and Alice Wallenberg Foundation, the Swedish Research Council (VR), and the Swedish Governmental Agency for Innovation Systems (VINNOVA) through the Berzelii Center EXSELENT. B.M.-M. also thanks VINNOVA for a VINNMER grant. A.E.P.-P. was supported by the MATsynCELL project, Röntgen-Ångström Cluster. L.S. was supported by the Consortium for Crystal Chemistry (C3), Röntgen-Ångström Cluster. The authors acknowledge the MAX IV Laboratory, Lund, for the use of the synchrotron facilities (Proposal 20120319). In particular, we thank Dr. Stefan Carlson for his assistance in using the I811 beamline.

Keywords: functionalisation · metal–organic frameworks · microporous materials · synthesis design · transition metal complexes

[1] a) G. Férey, *Chem. Soc. Rev.* **2008**, *37*, 191–214; b) O. M. Yaghi, M. O'Keeffe, N. W. Ockwig, H. K. Chae, M. Eddaoudi, J. Kim, *Nature* **2003**, *423*, 705–714.

[2] a) P. Horcajada, F. Salles, S. Wuttke, T. Devic, D. Heurtaux, G. Maurin, A. Vimont, M. Daturi, O. David, E. Magnier, N. Stock, Y. Filinchuk, D. Popov, C. Riekel, G. Férey, C. Serre, *J. Am. Chem. Soc.* **2011**, *133*, 17839–17847;

b) M. Eddaoudi, J. Kim, N. Rosi, D. Vodak, J. Wachter, M. O'Keeffe, O. M. Yaghi, *Science* **2002**, *295*, 469 – 472.

[3] a) J. F. Van Humbeck, T. M. McDonald, X. Jing, B. M. Wiers, G. Zhu, J. R. Long, *J. Am. Chem. Soc.* **2014**, *136*, 2432 – 2440; b) P. Valvekens, F. Vermoortele, D. De Vos, *Catal. Sci. Technol.* **2013**, *3*, 1435 – 1445; c) V. Pascanu, Q. Yao, A. Bermejo Gómez, M. Gustafsson, Y. Yun, W. Wan, L. Samain, X. Zou, B. Martín-Matute, *Chem. Eur. J.* **2013**, *19*, 17483 – 17493; d) A. E. Platero-Prats, N. Snejko, M. Iglesias, A. Monge, E. Gutiérrez-Puebla, *Chem. Eur. J.* **2013**, *19*, 15572 – 15582; e) P. Horcajada, T. Chalati, C. Serre, B. Gillet, C. Sebrie, T. Baati, J. F. Eubank, D. Heurtaux, P. Clayette, C. Kreuz, J.-S. Chang, Y. K. Hwang, V. Marsaud, P.-N. Bories, L. Cynober, S. Gil, G. Férey, P. Couvreur, R. Gref, *Nat. Mater.* **2010**, *9*, 172 – 178; f) N. L. Rosi, R. Eckert, M. Eddaoudi, D. T. Vodak, J. K. Kim, M. O'Keeffe, O. M. Yaghi, *Science* **2003**, *300*, 1127 – 1129.

[4] J. Hartwig, in *Organotransition Metal Chemistry: From Bonding to Catalysis*, (Ed.: H. Baltes), University Science Books, Sausalito, California, **2010**.

[5] a) Z. Wang, S. M. Cohen, *J. Am. Chem. Soc.* **2007**, *129*, 12368 – 12369; b) J. S. Seo, D. Whang, H. Lee, S. I. Jun, J. Oh, Y. J. Jeon, K. Kim, *Nature* **2000**, *404*, 982 – 986.

[6] H. Deng, C. J. Doonan, H. Furukawa, R. B. Ferreira, J. Towne, C. B. Knobler, B. Wang, O. M. Yaghi, *Science* **2010**, *327*, 846 – 850.

[7] a) O. Karagiaridi, W. Bury, J. E. Mondloch, J. T. Hupp, O. M. Farha, *Angew. Chem. Int. Ed.* **2014**, DOI: 10.1002/anie.201306923; *Angew. Chem.* **2014**, DOI: 10.1002/ange.201306923; b) T. Li, M. T. Kozlowski, E. A. Doud, M. N. Blakely, N. L. Rosi, *J. Am. Chem. Soc.* **2013**, *135*, 11688 – 11691; c) M. Kim, J. F. Cahill, Y. Su, K. A. Prather, S. M. Cohen, *Chem. Sci.* **2012**, *3*, 126 – 130.

[8] Selected examples: a) H. Fei, S. M. Cohen, *Chem. Commun.* **2014**, *50*, 4810 – 4812; b) W. Morris, B. Volosskiy, S. Demir, F. Gándara, P. L. McGrier, H. Furukawa, D. Cascio, J. F. Stoddart, O. M. Yaghi, *Inorg. Chem.* **2012**, *51*, 6443 – 6445; c) F. Carson, S. Agrawal, M. Gustafsson, A. Bartoszewics, F. Moraga, X. Zou, B. Martín-Matute, *Chem. Eur. J.* **2012**, *18*, 15337 – 15344; d) A. M. Shultz, A. A. Sarjeant, O. K. Farha, J. T. Hupp, S. T. Nguyen, *J. Am. Chem. Soc.* **2011**, *133*, 13252 – 13255; e) E. D. Bloch, D. Britt, C. Lee, C. J. Doonan, F. J. Uribe-Romo, H. Furukawa, J. R. Long, O. M. Yagui, *J. Am. Chem. Soc.* **2010**, *132*, 14382 – 14384; f) L. Ma, J. M. Falkowski, C. Abney, W. Lin, *Nat. Chem.* **2010**, *2*, 838 – 846.

[9] Selected examples: a) C. Wang, K. E. deKrafft, W. Lin, *J. Am. Chem. Soc.* **2012**, *134*, 7211 – 7214; b) F. Song, C. Wang, W. Lin, *Chem. Commun.* **2011**, *47*, 8256 – 8258; c) O. K. Farha, A. M. Shultz, A. A. Sarjeant, S. T. Nguyen, J. T. Hupp, *J. Am. Chem. Soc.* **2011**, *133*, 5652 – 5655; d) K. Oisaki, Q. Li, H. Furukawa, A. U. Czja, O. M. Yagui, *J. Am. Chem. Soc.* **2010**, *132*, 9262 – 9264; e) K. C. Szeto, K. P. Lillerud, M. Tilset, M. Bjørgen, C. Prestipino, A. Zecchina, C. Lamberti, S. Bordiga, *J. Phys. Chem. B* **2006**, *110*, 21509 – 21520; f) R. Kitaura, G. Onoyama, H. Sakamoto, R. Matsuda, S.-i. Noro, S. Kitagawa, *Angew. Chem. Int. Ed.* **2004**, *43*, 2684 – 2687; *Angew. Chem.* **2004**, *116*, 2738 – 2741.

[10] C. Wang, Z. Xie, K. E. deKrafft, W. Lin, *J. Am. Chem. Soc.* **2011**, *133*, 13445 – 13454.

[11] S. Pullen, H. Fei, A. Orthaber, S. M. Cohen, S. Ott, *J. Am. Chem. Soc.* **2013**, *135*, 16997 – 17003.

[12] J. H. Cavka, S. Jakobsen, U. Olsbye, N. Guillou, C. Lamberti, S. Bordiga, K. P. Lillerud, *J. Am. Chem. Soc.* **2008**, *130*, 13850 – 13851.

[13] Selected examples of similar complexes used in catalysis: a) N. Ahlsten, A. Bermejo Gómez, B. Martín-Matute, *Angew. Chem. Int. Ed.* **2013**, *52*, 6273 – 6276; *Angew. Chem.* **2013**, *125*, 6393 – 6396; b) S. Hansen, M. Klahn, T. Beweries, U. Rosenthal, *ChemSusChem* **2012**, *5*, 656 – 660; c) S. H. Lee, K. Won, H.-K. Song, C. B. Park, *Small* **2009**, *5*, 2162 – 2166.

[14] Recently, bpydc linkers have been proved to act as Lewis basic sites: L. Li, S. Tang, C. Wang, X. Lv, M. Jiang, H. Wu, X. Zhao, *Chem. Commun.* **2014**, *50*, 2304 – 2307.

[15] B. Ravel, M. Newville, *J. Synchrotron Radiat.* **2005**, *12*, 537 – 541.

[16] M. Newville, *J. Synchrotron Radiat.* **2001**, *8*, 322 – 324.

[17] B. Ravel, *J. Synchrotron Radiat.* **2001**, *8*, 314 – 316.

[18] J. Rehr, R. Albers, S. Zabinsky, *Phys. Rev. Lett.* **1992**, *69*, 3397 – 3400.

[19] G. S. Pawley, *J. Appl. Crystallogr.* **1981**, *14*, 357 – 361.

[20] We thank the referee for his/her suggestions.

Received: June 11, 2014
Published online on November 3, 2014